ICES REPORT 11-37

November 2011

Quadratic Serendipity Finite Elements on Polygons using Generalized Barycentric Coordinates

by

Alexander Rand, Andrew Gillette, and Chandrajit Bajaj

The Institute for Computational Engineering and Sciences
The University of Texas at Austin
Austin, Texas 78712

Reference: Alexander Rand, Andrew Gillette, and Chandrajit Bajaj , "Quadratic Serendipity Finite Elements on Polygon using Generalized Barycentric Coordinates", ICES REPORT 11-37, The Institute for Computational Engineering and Sciences, The University of Texas at Austin, November 2011.

MATHEMATICS OF COMPUTATION
Volume 00, Number 0, Pages 000–000
S 0025-5718(XX)0000-0

QUADRATIC SERENDIPITY FINITE ELEMENTS ON POLYGONS USING GENERALIZED BARYCENTRIC COORDINATES

ALEXANDER RAND, ANDREW GILLETTE, AND CHANDRAJIT BAJAJ

Abstract. We introduce a finite element construction for use on the class of convex, planar polygons and show it obtains a quadratic error convergence estimate. On a convex n-gon satisfying simple geometric criteria, our construction produces $2n$ basis functions, associated in a Lagrange-like fashion to each vertex and each edge midpoint, by transforming and combining a set of $n(n+1)/2$ basis functions known to obtain quadratic convergence. The technique broadens the scope of the so-called 'serendipity' elements, previously studied only for quadrilateral and regular hexahedral meshes, by employing the theory of generalized barycentric coordinates. Numerical evidence is provided on a trapezoidal quadrilateral mesh, previously not amenable to serendipity constructions, and applications to adaptive meshing are discussed.

1. Introduction

Barycentric coordinates provide a basis for linear finite elements on simplices, and generalized barycentric coordinates naturally produce a suitable basis for linear finite elements on general polygons. Various applications make use of this technique [14, 15, 24, 25, 26, 28, 30, 31, 32, 35], but in each case, only linear error estimates can be asserted. A quadratic finite element can easily be constructed by taking pairwise products of the basis functions from the linear element, yet this approach has not been pursued, primarily since the requisite number of basis functions grows quadratically in the number of vertices of the polygon. Still, many of the pairwise products are zero along the entire polygonal boundary and thus are unimportant for inter-element continuity, a key ingredient in the simplest finite element theory. For quadrilateral elements, these 'extra' basis functions are well understood and, for quadrilaterals that can be affinely mapped to a square, the so-called 'serendipity element' yields an acceptable basis consisting of only those basis functions needed to guarantee inter-element continuity [37, 4, 3]. We generalize this construction to produce a quadratic serendipity element for arbitrary convex polygons derived from generalized barycentric coordinates.

Our construction yields a set of Lagrange-like basis functions $\{\psi_{ij}\}$ – one per vertex and one per edge midpoint – using a linear combination of pairwise products of generalized barycentric functions $\{\lambda_i\}$. We show that this set spans all constant,

2010 *Mathematics Subject Classification.* Primary 65D05 65N30 41A30 41A25.
Key words and phrases. finite element, barycentric coordinates, serendipity.
This research was supported in part by NIH contracts R01-EB00487, R01-GM074258, and a grant from the UT-Portugal CoLab project.

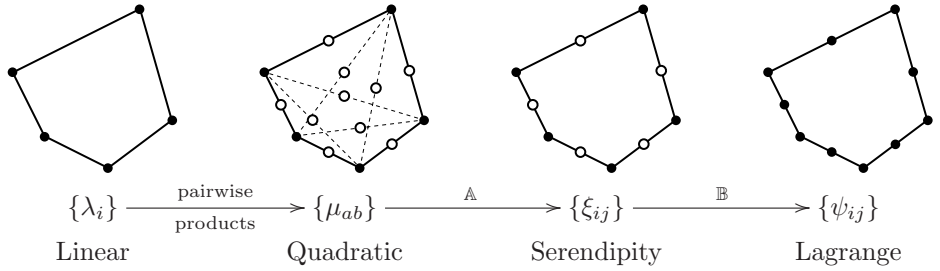

FIGURE 1. Overview of the construction process. In each figure, the dots are in one-to-one correspondence with the set of functions listed below it. At filled dots, all functions in the set evaluate to zero except for the function corresponding to the dot which evaluates to one. The rightmost element has quadratic precision with only these types of 'Lagrange-like' basis functions.

linear, and quadratic polynomials, making it suitable for finite element analysis via the Bramble-Hilbert lemma. Further, given uniform bounds on the aspect ratio, edge length, and interior angles of the polygon, we bound $||\psi_{ij}||_{H^1(\Omega)}$ uniformly with respect to $||\lambda_i||_{H^1(\Omega)}$, proving that the ψ_{ij} functions are well-behaved.

Figure 1 gives a visual depiction of the construction process. Starting with one generalized barycentric function λ_i per vertex of an n-gon, take all pairwise products yielding a total of $n(n+1)/2$ functions $\mu_{ab} := \lambda_a \lambda_b$. The linear transformation $\mathbb{A}$ reduces the set $\{\mu_{ab}\}$ to the $2n$ element set $\{\xi_{ij}\}$, indexed over vertices and edge midpoints of the polygon. A simple bounded linear transformation $\mathbb{B}$ converts $\{\xi_{ij}\}$ into a basis $\{\psi_{ij}\}$ which satisfies the "Lagrange property" meaning each function takes the value 1 at its associated node and 0 at all other nodes.

The paper is organized as follows. In Section 2 we review relevant background on finite element theory, generalized barycentric functions, and the serendipity element. In Section 3, we give the general version of our approach to defining $\mathbb{A}$, the reduction from a quadratic element to a serendipity element. In Section 4 we give the construction of $\mathbb{A}$ and its bounds in the special cases of regular polygons and convex quadrilaterals. In Section 5 we do the same for a generic polygon satisfying certain geometric constraints. In Section 6 we define $\mathbb{B}$ and show that the final $\{\psi_{ij}\}$ matrix is Lagrange-like. We describe practical applications and consider future directions in Section 7.

2. Background and Notation

Let Ω be a convex polygon with n vertices $(\mathbf{v}_1, \ldots, \mathbf{v}_n)$ ordered counter-clockwise. Denote the interior angle at $\mathbf{v}_i$ by β_i. The largest distance between two points in Ω (the diameter of Ω) is denoted $\operatorname{diam}(\Omega)$ and the radius of the largest inscribed circle is denoted $\rho(\Omega)$. The center of this circle is denoted $\mathbf{c}$ and is selected arbitrarily when no unique circle exists. The **aspect ratio** (or chunkiness parameter) γ is the ratio of the diameter to the radius of the largest inscribed circle, i.e.

$$\gamma := \frac{\operatorname{diam}(\Omega)}{\rho(\Omega)}.$$

The notation is shown in Figure 2.

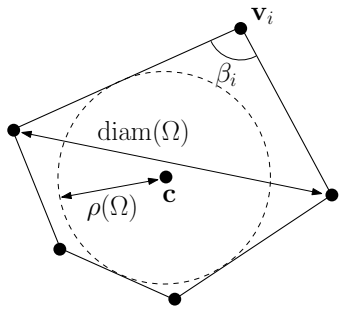

FIGURE 2. Notation used to describe polygonal geometry.

For a multi-index $\alpha = (\alpha_1, \alpha_2)$ and point $\mathbf{x} = (x, y)$, define $\mathbf{x}^\alpha := x^{\alpha_1} y^{\alpha_2}$, $\alpha! := \alpha_1 \alpha_2$, $|\alpha| := \alpha_1 + \alpha_2$, and $D^\alpha u := \partial^{|\alpha|} u / \partial x^{\alpha_1} \partial y^{\alpha_2}$. The Sobolev semi-norms and norms over an open set Ω are defined by

$$|u|^2_{H^m(\Omega)} := \int_\Omega \sum_{|\alpha|=m} |D^\alpha u(\mathbf{x})|^2 \, \mathrm{d}\mathbf{x} \quad \text{and} \quad ||u||^2_{H^m(\Omega)} := \sum_{0 \le k \le m} |u|^2_{H^k(\Omega)} .$$

The H^0-norm is the L^2-norm and will be denoted $||\cdot||_{L^2(\Omega)}$. The space of polynomials of degree $\le k$ on a domain is denoted $\mathcal{P}_k$.

2.1. **The Bramble-Hilbert Lemma.** A finite element method approximates a function u from an infinite-dimensional functional space V by a function u_h from a finite-dimensional subspace $V_h \subset V$. The goal of such approaches is to prove that the error of the numerical solution u_h is bounded *a priori* by the error of the best approximation available in V_h, i.e. $||u - u_h||_V \le C \inf_{w \in V_h} ||u - w||_V$. In this paper, $V = H^1$ and V_h is a set of functions defined piecewise over a 2D mesh of convex polygons. The parameter h indicates the maximum diameter of an element in the mesh. Further details on the finite element method can be found in a number of textbooks [7, 5, 10, 37].

A quadratic finite element method in this context means that when $h \to 0$, the best approximation error $(\inf_{w \in V_h} ||u - w||_V)$ converges to zero with order h^2. This means the space V_h is 'dense enough' in V to allow for quadratic convergence. Such arguments are usually proved via the Bramble-Hilbert lemma which guarantees that if V_h contains polynomials up to a certain degree, a bound on the approximation error can be found. The variant of the Bramble-Hilbert lemma stated below includes a uniform constant over all convex domains which is a necessary detail in the context of general polygonal elements and generalized barycentric functions.

Lemma 2.1 (Bramble-Hilbert [33, 9])**.** *There exists a uniform constant C_{BH} such that for all convex polygons Ω and for all $u \in H^k(\Omega)$, there exists a degree k polynomial p_u with $||u - p_u||_{H^{k'}(\Omega)} \le C_{BH} \operatorname{diam}(\Omega)^{k+1-k'} |u|_{H^{k+1}(\Omega)}$ for any $k' \le k$.*

Our focus is on quadratic elements (i.e., $k = 2$) and error estimates in the H^1-norm (i.e., $k' = 1$) which yields an estimate that scales with $\operatorname{diam}(\Omega)^2$. Our methods extend to more general (i.e., $W^{k,p}$) spaces whenever the Bramble-Hilbert lemma holds. Extensions to higher order elements ($k > 2$) will be briefly discussed in Section 7.

Observe that if Ω is transformed by any invertible affine map T, the polynomial $p \circ T^{-1}$ on $T\Omega$ has the same degree as the polynomial p on Ω. This fact is often exploited in the simpler and well-studied case of triangular meshes; an estimate on a reference triangle $\hat{K}$ becomes an estimate on any physical triangle K by passing through an affine transformation taking $\hat{K}$ to K. For $n > 3$, however, two generic n-gons may differ by a non-affine transformation and thus, as we will see in the next section, the use of a single reference element can become overly restrictive on element geometry. In our arguments, we instead use a class of reference elements, namely, convex polygons of diameter one satisfying the geometric criteria given in Section 2.3.

2.2. **Serendipity Quadratic Elements.** The term 'serendipity element' refers to a long-standing observation in the finite element community that tensor product bases of polynomials on rectangular meshes of quadrilaterals in 2D or cubes in 3D can obtain higher order convergence rates with fewer than the 'expected' number of basis functions resulting from tensor products. This phenomenon is discussed in many finite element textbooks, e.g. [29, 19, 7], and was recently characterized precisely by Arnold and Awanou [3]. For instance, the degree k tensor product basis on a square reference element has $(k+1)^2$ basis functions and can have guaranteed convergence rates of order $k+1$ when transformed to a rectangular mesh via bilinear isomorphisms [4]. By the Bramble-Hilbert lemma, however, the function space spanned by this basis may be unnecessarily large as the dimension of $\mathcal{P}_k$ is only $(k+1)(k+2)/2$ and only $4k$ degrees of freedom associated to the boundary are needed to ensure sufficient inter-element continuity in H^1.

This motivates the construction of the serendipity element for quadrilaterals. By a judicious choice of basis functions, an order $k+1$ convergence rate can be obtained with only $4k$ basis functions associated with the edges of the quadrilateral and q additional functions associated with interior points where $q = 0$ when $k < 4$ [3]. Such an approach only works if the reference element is mapped via an affine transformation; it has been demonstrated that the serendipity element fails on trapezoidal elements, such as those shown in Figure 8 [23, 21, 37, 36].

Some very specific serendipity elements have been constructed for quadrilaterals and regular hexagons based on the Wachspress coordinates (discussed in the next sections) [34, 2, 17, 1, 18]. Our work generalizes this construction to arbitrary polygons without dependence on the type of generalized barycentric coordinate selected and with uniform bounds under certain geometric criteria.

2.3. **Generalized Barycentric Elements.** To avoid non-affine transformations associated with tensor products constructions on a single reference element, we use generalized barycentric coordinates to define our basis function. These coordinates are any functions satisfying the following agreed-upon definition in the literature.

Definition 2.2. Functions $\lambda_i : \Omega \to \mathbb{R}$, $i = 1, \ldots, n$ are **barycentric coordinates** on Ω if they satisfy two properties.

B1. **Non-negative**: $\lambda_i \geq 0$ on Ω.

B2. **Linear Completeness**: For any linear function $L : \Omega \to \mathbb{R}$, $L = \sum_{i=1}^{n} L(\mathbf{v}_i)\lambda_i$.

We will further restrict our attention to barycentric coordinates satisfying the following invariance property. Let $T : \mathbb{R}^2 \to \mathbb{R}^2$ be a composition of translation, rotation, and uniform scaling transformations and let $\{\lambda_i^T\}$ denote a set of barycentric coordinates on $T\Omega$.

B3. **Invariance:** $\lambda_i(\mathbf{x}) = \lambda_i^T(T(\mathbf{x}))$.

This assumption will allow estimates over the class of convex sets with diameter one to be immediately extended to generic sizes since translation, rotation and uniform scaling operations can be easily passed through Sobolev norms. At the expense of requiring uniform bounds over a class of diameter-one domains rather than a single reference element, we avoid having to handle non-affine mappings between reference and physical elements.

A set of barycentric coordinates $\{\lambda_i\}$ also satisfies three additional familiar properties. A proof that B1 and B2 imply the additional properties B4-B6 can be found in [16].

B4. **Partition of unity:** $\sum_{i=1}^{n} \lambda_i \equiv 1$.

B5. **Linear precision:** $\sum_{i=1}^{n} \mathbf{v}_i \lambda_i(\mathbf{x}) = \mathbf{x}$.

B6. **Interpolation:** $\lambda_i(\mathbf{v}_j) = \delta_{ij}$.

Various particular barycentric coordinates have been constructed in the literature. We briefly mention a few of the more prominent kinds and associated references here; readers are referred to our prior work [16, Section 2] as well as the survey papers of Cueto et al. [8] and Sukumar and Tabarraei [31] for further details. The triangulation coordinates λ^{Tri} are defined by triangulating the polygon and using the standard barycentric coordinates over each triangle [13]. Harmonic coordinates λ^{Har} are defined as the solution to Laplace's equation on the polygon with linear boundary data satisfying B6 [20, 24, 6]. Explicitly constructed functions include the rational Wachspress coordinates λ^{Wach} [34], the Sibson coordinates λ^{Sibs} defined in terms of the Voronoi diagram of the vertices of the polygon [27, 11], and the mean value coordinates λ^{MVal} defined by Floater [12, 13].

To obtain convergence estimates with any of these functions, certain geometric conditions must be satisfied by a generic mesh element. We will consider domains satisfying the following three geometric conditions.

G1. **Bounded aspect ratio:** There exists $\gamma^* \in \mathbb{R}$ such that $\gamma < \gamma^*$.

G2. **Minimum edge length:** There exists $d_* \in \mathbb{R}$ such that $|\mathbf{v}_i - \mathbf{v}_j| > d_* > 0$ for all $i \neq j$.

G3. **Maximum interior angle:** There exists $\beta^* \in \mathbb{R}$ such that $\beta_i < \beta^* < \pi$ for all i.

Under some set of these conditions, the H^1-norm of many generalized barycentric coordinates are bounded which is the key estimate in asserting the expected (linear) convergence rate in the typical finite element setting.

Theorem 2.3 ([16])**.** *For any convex domain Ω satisfying G1, G2, and G3, the triangulation, harmonic, Wachspress, and Sibson coordinates are all bounded in H^1; i.e., there exists a constant $C > 0$ such that*

$$||\lambda_i||_{H^1(\Omega)} \leq C. \tag{2.1}$$

The results in [16] are somewhat stronger than the statement of Theorem 2.3, namely, not all of the geometric hypotheses are necessary for every coordinate construction. Our results, however, rely generically on any set of barycentric coordinates satisfying (2.1). Any additional dependence on the shape geometry will be made explicitly clear in the proofs.

2.4. **Quadratic Precision Barycentric Functions.** Since generalized barycentric coordinates are only guaranteed to have linear precision (B5), they cannot provide greater than linear order error estimates. Langer and Seidel have considered a higher order barycentric interpolation [22] in the computer graphics literature but seek to satisfy different axioms than we desire in the finite element setting: namely, their approach is designed to produce a smoother (C^1) global interpolant but does not attempt to span higher-order polynomial spaces. By taking products of λ_i functions, however, we can obtain a quadratic precision property and ensure second order error estimates.

Proposition 2.4. Given a set of barycentric coordinates $\{\lambda_i\}$, the set of functions $\{\mu_{ab}\} := \{\lambda_a \lambda_b\}$ has constant, linear, and quadratic precision[1], i.e.

$$\sum_{ab} \mu_{ab} = 1, \qquad \sum_{ab} \mathbf{v}_a \mu_{ab} = \mathbf{x} \qquad \text{and} \qquad \sum_{ab} \mathbf{v}_a \mathbf{v}_b^T \mu_{ab} = \mathbf{x}\mathbf{x}^T. \tag{2.2}$$

Proof. The result is immediate from properties B4 and B5 of the λ_i functions. □

Since $\mu_{ab} = \mu_{ba}$, the summations from (2.2) can be written in a symmetric expansion which will help motivate our definition of a serendipity element. We will use the abbreviated notation

$$\mathbf{v}_{ab} := \frac{\mathbf{v}_a + \mathbf{v}_b}{2},$$

so that $\mathbf{v}_{aa}$ is just a different expression for $\mathbf{v}_a$.

Q1. **Constant Precision**: $\displaystyle\sum_a \mu_{aa} + \sum_{a<b} 2\mu_{ab} = 1$

Q2. **Linear Precision**: $\displaystyle\sum_a \mathbf{v}_{aa}\mu_{aa} + \sum_{a<b} 2\mathbf{v}_{ab}\mu_{ab} = \mathbf{x}$

Q3. **Quadratic Precision**: $\displaystyle\sum_a \mathbf{v}_a \mathbf{v}_a^T \mu_{aa} + \sum_{a<b} (\mathbf{v}_a \mathbf{v}_b^T + \mathbf{v}_b \mathbf{v}_a^T)\mu_{ab} = \mathbf{x}\mathbf{x}^T$

Finally, the product rule ensures that Theorem 2.3 extends immediately to the pairwise product functions.

Corollary 2.5. *For any convex domain Ω satisfying G1, G2, and G3, pairwise products of the triangulation, harmonic, Wachspress, and Sibson coordinates are all bounded in H^1; i.e., there exists a constant $C > 0$ such that*

$$||\mu_{ab}||_{H^1(\Omega)} \leq C. \tag{2.3}$$

[1]Note that $\mathbf{x}\mathbf{x}^T$ is a symmetric matrix of quadratic monomials.

3. Constructing Serendipity Elements from Quadratic Elements

We construct a serendipity quadratic element with basis functions $\{\xi_{ij}\}$ by taking a linear transformation of the generic quadratic element basis $\{\mu_{ab}\}$. For a polygon with n vertices, we fix the orderings:

$$\{\mu_{11}, \mu_{22}, \ldots, \mu_{nn}, \mu_{12}, \mu_{23}, \ldots, \mu_{(n-1)n}, \mu_{1n}, \mu_{13}, \ldots, (\text{lexicographical}), \ldots, \mu_{(n-2)n}\};$$

$$\{\xi_{11}, \xi_{22}, \ldots, \xi_{nn}, \xi_{12}, \xi_{23}, \ldots, \xi_{(n-1)n}, \xi_{1n}\}.$$

Note that these ordered bases agree on the indices of the first $2n$ elements and the remaining μ_{ab} functions satisfy $b - a > 1$. The ξ_{ij} basis is defined as the image of a linear transformation $\mathbb{A} : \mathbb{R}^{n(n+1)/2} \to \mathbb{R}^{2n}$ such that

$$\mathbb{A}[\mu_{ab}] = [\xi_{ij}] \tag{3.1}$$

on the orderings defined above. We will write $\mathbb{A}$ as a matrix with entries c_{ab}^{ij}, where ab and ij are the indices of the corresponding μ_{ab} and ξ_{ij} functions for that entry. Hence the structure of $\mathbb{A}$ with respect to indices is

$$\mathbb{A} := \left[\begin{array}{c|c|c} c_{aa}^{ii} & c_{a(a+1)}^{ii} & c_{ab}^{ij} \\ \hline c_{aa}^{i(i+1)} & c_{a(a+1)}^{i(i+1)} & \end{array}\right]. \tag{3.2}$$

The first two columns in this decomposition are composed of two $n \times n$ sub-matrices. The last column contains those c_{ab}^{ij} with $j \in \{i, i+1\}$ and $b - a > 1$. There are $(n^2 + n)/2$ functions $\{\mu_{ab}\}$ (n functions of the form μ_{aa} plus $\binom{n}{2}$ functions of the form μ_{ab} with $a \neq b$, and thus the last component in (3.2) is a $2n \times ((n^2 - 3n)/2)$ sub-matrix.

While the coefficients of $\mathbb{A}$ could be fixed according to a variety of heuristics, we choose to set them in such a way that the resulting ξ_{ij} functions satisfy constraints analogous to Q1, Q2, and Q3. First we state precisely the constraints we plan to enforce.

$\mathrm{Q}_\xi 1$. **Constant Precision**: $\displaystyle\sum_i \xi_{ii} + 2\xi_{i(i+1)} = 1$.

$\mathrm{Q}_\xi 2$. **Linear Precision**: $\displaystyle\sum_i \mathbf{v}_{ii}\xi_{ii} + 2\mathbf{v}_{i(i+1)}\xi_{i(i+1)} = \mathbf{x}$.

$\mathrm{Q}_\xi 3$. **Quadratic Precision**: $\displaystyle\sum_i \mathbf{v}_i\mathbf{v}_i^T\xi_{ii} + (\mathbf{v}_i\mathbf{v}_{i+1}^T + \mathbf{v}_{i+1}\mathbf{v}_i^T)\xi_{i(i+1)} = \mathbf{x}\mathbf{x}^T$.

Substituting $\xi_{ij} = \sum_{a \leq b} c_{ab}^{ij}\mu_{ab}$ from (3.1) into $\mathrm{Q}_\xi 1$-$\mathrm{Q}_\xi 3$ gives constraints on the entries c_{ab}^{ij}. For instance, $\mathrm{Q}_\xi 1$ becomes

$$\sum_i \left(\sum_{a \leq b} c_{ab}^{ii}\mu_{ab}\right) + 2\left(\sum_{a \leq b} c_{ab}^{i(i+1)}\mu_{ab}\right) = 1.$$

After swapping the order of summation and regrouping, this is

$$\sum_a \left(\sum_i c_{aa}^{ii} + 2c_{aa}^{i(i+1)}\right)\mu_{aa} + \sum_{a<b}\left(\sum_i c_{ab}^{ii} + 2c_{ab}^{i(i+1)}\right)\mu_{ab} = 1. \tag{3.3}$$

Matching coefficients between (3.3) and Q1, we derive the constraints

$$\sum_i c_{aa}^{ii} + 2c_{aa}^{i(i+1)} = 1 \quad \text{and} \quad \sum_i c_{ab}^{ii} + 2c_{ab}^{i(i+1)} = 2, \text{ for } a < b.$$

Carrying out this process of substitution, regrouping, and matching coefficients for $Q_\xi 2$ and $Q_\xi 3$, we can rewrite the constraints as follows.

$Q_\xi 1$. **Constant Precision**: $\sum_i c_{aa}^{ii} + 2c_{aa}^{i(i+1)} = 1$ and

$$\sum_i c_{ab}^{ii} + 2c_{ab}^{i(i+1)} = 2, \text{ for } a < b. \tag{3.4}$$

$Q_\xi 2$. **Linear Precision**: $\sum_i c_{aa}^{ii}\mathbf{v}_{ii} + 2c_{aa}^{i(i+1)}\mathbf{v}_{i(i+1)} = \mathbf{v}_{aa}$ and

$$\sum_i c_{ab}^{ii}\mathbf{v}_{ii} + 2c_{ab}^{i(i+1)}\mathbf{v}_{i(i+1)} = 2\mathbf{v}_{ab}, \text{ for } a < b \tag{3.5}$$

$Q_\xi 3$. **Quadratic Precision**: $\sum_i c_{aa}^{ii}\mathbf{v}_i\mathbf{v}_i^T + c_{aa}^{i(i+1)}(\mathbf{v}_i\mathbf{v}_{i+1}^T + \mathbf{v}_{i+1}\mathbf{v}_i^T) = \mathbf{v}_a\mathbf{v}_a^T$ and

$$\sum_i c_{ab}^{ii}\mathbf{v}_i\mathbf{v}_i^T + c_{ab}^{i(i+1)}(\mathbf{v}_i\mathbf{v}_{i+1}^T + \mathbf{v}_{i+1}\mathbf{v}_i^T) = \mathbf{v}_a\mathbf{v}_b^T + \mathbf{v}_b\mathbf{v}_a^T, \text{ for } a < b. \tag{3.6}$$

Observe that the first equation in each constraint involves only coefficients in the first block column of the decomposition of $\mathbb{A}$ given in (3.2). We satisfy these equations by setting

$$c_{aa}^{ii} := \delta_{ia} \quad \text{and} \quad c_{aa}^{i(i+1)} := 0.$$

For the second equation in each constraint, we first address the case of $b = a + 1$. This corresponds to coefficients within a single column of the second block column of the decomposition of $\mathbb{A}$ given in (3.2). We satisfy these equations in a similar fashion by setting

$$c_{a(a+1)}^{ii} := 0 \quad \text{and} \quad c_{a(a+1)}^{i(i+1)} := \delta_{ia}.$$

Summarizing so far, $\mathbb{A}$ has the form

$$\mathbb{A} := \left[\begin{array}{c|c|c} \mathbb{I} & 0 & \\ \hline 0 & \mathbb{I} & \mathbb{A}' \end{array}\right]. \tag{3.7}$$

where $\mathbb{I}$ is the $n \times n$ identity matrix, leaving the sub-matrix $\mathbb{A}'$ still to be defined. The coefficients of $\mathbb{A}'$ describe how the μ_{ab} interior basis functions (i.e., those associated to a pair of distinct, non-adjacent vertices of the polygon) are incorporated into the definition of the ξ_{ij} functions. We discuss how these coefficients can be set in the special cases of regular polygons and quadrilaterals before addressing the generic polygon.

In each case, we will show that $\mathbb{A}$ is bounded in the maximum absolute row sum norm, i.e.

$$||\mathbb{A}|| := \max_{ij} \sum_{ab} |c_{ab}^{ij}|. \tag{3.8}$$

This norm gives an immediate bound on the H^1 norm of the ξ functions since (3.1) and (2.3) imply

$$||\xi_{ij}||_{H^1(\Omega)} \leq ||\mathbb{A}|| \max_{ab} ||\mu_{ab}||_{H^1(\Omega)} < C||\mathbb{A}||.$$

Finally, since the space of linear transformations from $\mathbb{R}^{n(n+1)/2}$ to $\mathbb{R}^{2n}$ is finite-dimensional and thus all norms on $\mathbb{A}$ are equivalent, a bound on the coefficients of $\mathbb{A}'$ is sufficient to bound $||\mathbb{A}||$.

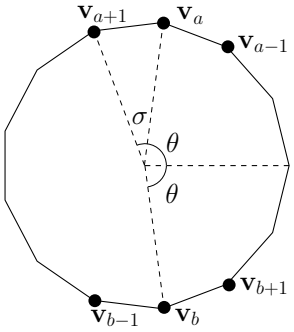

FIGURE 3. Notation for the construction for a regular polygon.

4. Special Cases

Before giving a general construction of the coefficients in $\mathbb{A}'$, we study some simpler special cases in which symmetry reduces the number of equations that must be satisfied simultaneously.

4.1. **Regular Polygons.** For simplicity, we consider the construction for regular polygons. We consider two generic non-adjacent vertices $\mathbf{v}_a$ and $\mathbf{v}_b$. Without loss of generality, this configuration can be described by two parameters $0 < \sigma \leq \theta \leq \pi/2$ as in Figure 3. Note that the n vertices of the polygon are located at angles of the form $k\sigma$ where $k = 0, 1, \ldots, n-1$. The coordinates of the six vertices of importance are:

$$\mathbf{v}_a = \begin{bmatrix}\cos\theta\\ \sin\theta\end{bmatrix}; \qquad \mathbf{v}_{a-1} = \begin{bmatrix}\cos(\theta-\sigma)\\ \sin(\theta-\sigma)\end{bmatrix}; \qquad \mathbf{v}_{a+1} = \begin{bmatrix}\cos(\theta+\sigma)\\ \sin(\theta+\sigma)\end{bmatrix};$$
$$\mathbf{v}_b = \begin{bmatrix}\cos\theta\\ -\sin\theta\end{bmatrix}; \qquad \mathbf{v}_{b-1} = \begin{bmatrix}\cos(\theta+\sigma)\\ -\sin(\theta+\sigma)\end{bmatrix}; \qquad \mathbf{v}_{b+1} = \begin{bmatrix}\cos(\theta-\sigma)\\ -\sin(\theta-\sigma)\end{bmatrix}.$$

We seek to establish the existence of suitable constants c_{ab}^{aa}, $c_{ab}^{a,a+1}$, $c_{ab}^{a-1,a}$, c_{ab}^{bb}, $c_{ab}^{b-1,b}$, $c_{ab}^{b,b+1}$ which preserve quadratic precision and to investigate the geometric conditions under which these constants become large. The symmetry of this configuration suggests that $c_{ab}^{aa} = c_{ab}^{bb}$, $c_{ab}^{a-1,a} = c_{ab}^{b,b+1}$, and $c_{ab}^{a,a+1} = c_{ab}^{b-1,b}$ are reasonable requirements. For simplicity we will denote these constants by $c_0 := c_{ab}^{aa}$, $c_- := c_{ab}^{a-1,a}$, and $c_+ := c_{ab}^{a,a+1}$.

The constant precision requirement leads to the equation,

$$2c_0 + 4c_- + 4c_+ = 2. \tag{4.1}$$

Linear precision involves two requirements, one of which is trivially satisfied in our symmetric configuration. Thus, the only restriction that we must be careful to maintain is

$$2\cos\theta c_0 + 2\left[\cos\theta + \cos(\theta-\sigma)\right]c_- + 2\left[\cos\theta + \cos(\theta+\sigma)\right]c_+ = 2\cos\theta. \tag{4.2}$$

Quadratic precision involves three more requirements, one of which is again trivially satisfied. This gives two remaining restrictions:

$$2\cos^2\theta c_0 + 4\cos\theta\cos(\theta-\sigma)c_- + 4\cos\theta\cos(\theta+\sigma)c_+ = 2\cos^2\theta; \tag{4.3}$$

$$2\sin^2\theta c_0 + 4\sin\theta\sin(\theta-\sigma)c_- + 4\sin\theta\sin(\theta+\sigma)c_+ = -2\sin^2\theta. \tag{4.4}$$

Now we have four equations (4.1)-(4.4) and three unknowns c_0, c_- and c_+. Fortunately, equation (4.2) is a simple linear combination of (4.1) and(4.3); specifically (4.2) is $\frac{\cos\theta}{2}$ times (4.1) plus $\frac{1}{2\cos\theta}$ times (4.3). With a little algebra, we can produce the system:

$$\begin{bmatrix} 1 & 2 & 2 \\ 1 & 2(\cos\sigma + \sin\sigma\tan\theta) & 2(\cos\sigma - \sin\sigma\tan\theta) \\ 1 & 2(\cos\sigma - \sin\sigma\cot\theta) & 2(\cos\sigma + \sin\sigma\cot\theta) \end{bmatrix} \begin{bmatrix} c_0 \\ c_- \\ c_+ \end{bmatrix} = \begin{bmatrix} 1 \\ 1 \\ -1 \end{bmatrix}. \tag{4.5}$$

The solution of this system can be computed:

$$c_0 = \frac{(-1+\cos\sigma)\cot\theta + (1+\cos\sigma)\tan\theta}{(-1+\cos\sigma)(\cot\theta+\tan\theta)};$$

$$c_- = \frac{\cos\sigma - \sin\sigma\tan\theta - 1}{2\,(\tan\theta+\cot\theta)\sin\sigma\,(\cos\sigma-1)}; \quad c_+ = \frac{1-\cos\sigma-\sin\sigma\tan\theta}{2\,(\tan\theta+\cot\theta)\sin\sigma\,(\cos\sigma-1)}.$$

Although $\tan\theta$ (and thus the solution above) is not defined for $\theta = \pi/2$, the solution in this boundary case can be defined by the limiting value which always exists. By construction, we have the following lemma.

Lemma 4.1. *The coefficients c_0, c_-, c_+ satisfy constraints $Q_\xi 1$-$Q_\xi 3$.*

Finally, it remains to verify that the matrix $\mathbb{A}$ is bounded for our construction.

Theorem 4.2. *Let $\mathbb{A}_n$ denote the matrix $\mathbb{A}$ for a regular n-gon. Then $||\mathbb{A}_n||$ is uniformly bounded by a constant depending only on n.*

Proof. By the definition of $||\mathbb{A}||$ in (3.8), it suffices to bound the entries of $\mathbb{A}_n$ with respect to n. Note that $\sigma := 2\pi/n$ and recall that $\theta = k\sigma$ where k is a positive integer such that $\theta \le \pi/2$. We set k^* to be the largest integer k satisfying $k^*\sigma < \pi/2$. Define lower and upper bounds T_* and T^* by

$$0 < T_* := \tan\sigma \le \tan\theta \le \tan k^*\sigma =: T^* < \infty.$$

Note T^* and T_* depend only on n since $\sigma = 2\pi/n$. Also note

$$0 < \frac{1}{T^*} = \cot k^*\sigma \le \cot\theta \le \cot\sigma = \frac{1}{T_*} < \infty.$$

First we bound c_0:

$$|c_0| \le \frac{(1+\cos(2\pi/n))(T^* + 1/T_*)}{(1-\cos(2\pi/n))(T_* + 1/T^*)}.$$

For the other two coefficients, we have

$$|c_-|, |c_+| \le \frac{\cos(2\pi/n) + \sin(2\pi/n)T^* + 1}{|2(T_* + 1/T^*)\sin(2\pi/n)(\cos(2\pi/n)-1)|}. \qquad \square$$

We observe that the bounds on c_0, c_- and c_+ grow large as σ goes toward zero, i.e., when n gets large. For any fixed n, however, the bounds are always finite.

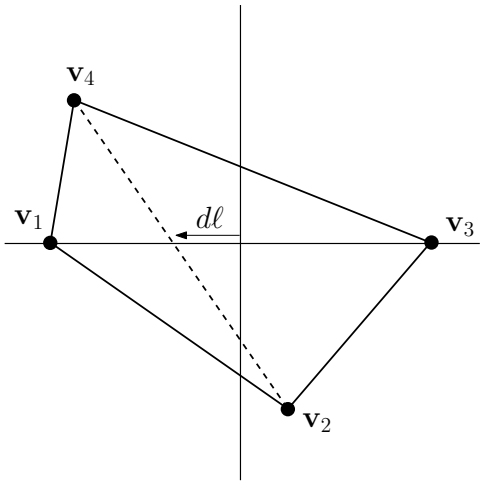

FIGURE 4. A generic convex quadrilateral, rotated so that one of its diagonals lies on the x-axis.

4.2. **Generic Quadrilaterals.** Fix a convex quadrilateral Ω with vertices $\mathbf{v}_1$, $\mathbf{v}_2$, $\mathbf{v}_3$, and $\mathbf{v}_4$, ordered counterclockwise. It suffices to describe how to set the coefficients c_{13}^{ij}. Without loss of generality, suppose that $\mathbf{v}_1 := (-\ell, 0)$ and $\mathbf{v}_3 := (\ell, 0)$ so that $\mathbf{v}_2$ is below the x-axis and $\mathbf{v}_4$ is above the x-axis, as shown in Figure 4. We have eight coefficients to set:

$$c_{13}^{11},\ c_{13}^{22},\ c_{13}^{33},\ c_{13}^{44},\ c_{13}^{12},\ c_{13}^{23},\ c_{13}^{34},\ \text{and}\ c_{13}^{14}.$$

Using a subscript x or y to denote the corresponding component of a vertex, define the coefficients as follows.

$$c_{13}^{22} := 0 \qquad c_{13}^{44} := 0 \tag{4.6}$$

$$c_{13}^{12} := \frac{(\mathbf{v}_4)_y}{(\mathbf{v}_4)_y - (\mathbf{v}_2)_y} \qquad c_{13}^{34} := \frac{(\mathbf{v}_2)_y}{(\mathbf{v}_2)_y - (\mathbf{v}_4)_y} \tag{4.7}$$

$$c_{13}^{23} := c_{13}^{12} \qquad c_{13}^{14} := c_{13}^{34} \tag{4.8}$$

$$c_{13}^{11} := \frac{c_{13}^{12}(\mathbf{v}_2)_x + c_{13}^{34}(\mathbf{v}_4)_x}{\ell} - 1 \quad c_{13}^{33} := -\frac{c_{13}^{12}(\mathbf{v}_2)_x + c_{13}^{34}(\mathbf{v}_4)_x}{\ell} - 1 \tag{4.9}$$

We observe that a uniform scaling of the domain does not change the coefficients, i.e., our restriction to domains of diameter one is without loss of generality. For ease of notation in the rest of this section, we define the quantity

$$d := \frac{c_{13}^{12}(\mathbf{v}_2)_x + c_{13}^{34}(\mathbf{v}_4)_x}{\ell}.$$

First we assert that the resulting basis does have quadratic precision.

Lemma 4.3. *The coefficients given in (4.6)-(4.9) satisfy constraints $Q_\xi 1$-$Q_\xi 3$.*

Proof. The proof is carried out by plugging the values from (4.6)-(4.9) into the constraints $\mathrm{Q}_\xi 1$-$\mathrm{Q}_\xi 3$ as given in (3.4)-(3.6) in the case $a = 1$, $b = 3$. First note that

$$c_{13}^{11} + c_{13}^{33} = -2 \quad \text{and} \quad c_{13}^{11} - c_{13}^{33} = 2d. \tag{4.10}$$

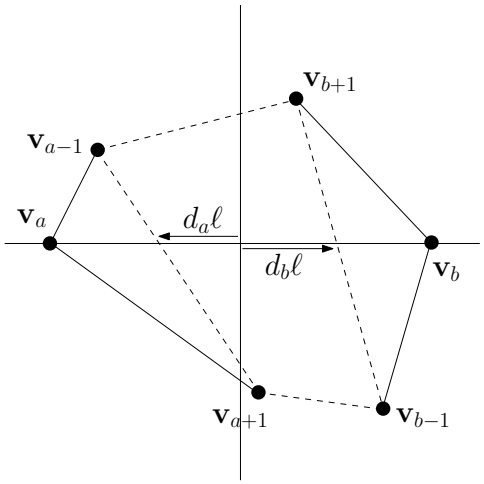

FIGURE 5. Generic convex polygon, rotated so that $\mathbf{v}_a = (-\ell, 0)$ and $\mathbf{v}_b = (\ell, 0)$. The x-intercept of the line between $\mathbf{v}_{a-1}$ and $\mathbf{v}_{a+1}$ is defined to be $-d_a\ell$ and the x-intercept of the line between $\mathbf{v}_{b-1}$ and $\mathbf{v}_{b+1}$ is defined to be $d_b\ell$.

For $\mathrm{Q}_\xi 1$, the sum reduces to

$$c_{13}^{11} + c_{13}^{33} + 4(c_{13}^{12} + c_{13}^{34}) = -2 + 4(1) = 2,$$

as required. For $\mathrm{Q}_\xi 2$, the x-coordinate equation reduces to

$$\ell(c_{13}^{33} - c_{13}^{11}) + 2d\ell = 0$$

which reduces to $0 = 0$ by (4.10). The y-coordinate equation reduces to $2(c_{13}^{12}(\mathbf{v}_2)_y + c_{13}^{34}(\mathbf{v}_4)_y) = 0$ which holds by (4.7). Finally, a bit of algebra reduces the matrix equality of $\mathrm{Q}_\xi 3$ to only the equality $\ell^2(c_{13}^{11} + c_{13}^{33}) = -2\ell^2$ of its first entry, which holds by (4.10). □

Theorem 4.4. *Given a convex quadrilateral, $||\mathbb{A}||$ is uniformly bounded.*

Proof. By the structure of $\mathbb{A}$ from (3.7) and definition of $||\mathbb{A}||$ in (3.8), it suffices to bound $|c_{13}^{ij}|$ uniformly. First observe convex combinations of the vertices $\mathbf{v}_2$ and $\mathbf{v}_4$ using coefficients c_{13}^{12} and c_{13}^{34} produces a point lying on the x-axis, i.e.,

$$1 = c_{13}^{12} + c_{13}^{34}, \text{ and} \tag{4.11}$$

$$0 = c_{13}^{12}(\mathbf{v}_2)_y + c_{13}^{34}(\mathbf{v}_4)_y. \tag{4.12}$$

Since $(\mathbf{v}_2)_y > 0$ and $(\mathbf{v}_4)_y < 0$, it follows that $c_{13}^{12}, c_{13}^{34} \in (0, 1)$. By (4.8), it also follows that $c_{13}^{23}, c_{13}^{14} \in (0, 1)$.

For c_{13}^{11} and c_{13}^{33}, note that the quantity $d\ell$ is the x-intercept of the line segment connecting $\mathbf{v}_2$ and $\mathbf{v}_4$. Thus $d\ell \in [-\ell, \ell]$ by convexity. So $d \in [-1, 1]$. Hence $|c_{13}^{11}| = |d - 1| \leq 2$ and $|c_{13}^{33}| = |-d - 1| \leq 2$. □

5. Generic Polygons

We now define the sub-matrix $\mathbb{A}'$ from (3.7) in the case of a generic polygon. Pick a column of $\mathbb{A}'$, i.e., fix an ab pair with $b - a > 1$. The coefficients c_{ab}^{ij} are

constrained by a total of six equations: one from $\mathrm{Q}_\xi 1$, two from $\mathrm{Q}_\xi 2$, and three from $\mathrm{Q}_\xi 3$ (since the symmetric matrix $\mathbf{x}\mathbf{x}^T$ is defined by only three parameters). This means at most six c_{ab}^{ij} coefficients are required to enforce the constraints and the rest can be set to zero. We define

$$c_{ab}^{ii} := 0, \text{ for } i \notin \{a, b\} \quad \text{and} \quad c_{ab}^{i(i+1)} = 0, \text{ for } i \notin \{a-1, a, b-1, b\},$$

leaving only the following six coefficients to be determined:

$$c_{ab}^{aa},\ c_{ab}^{bb},\ c_{ab}^{(a-1)a},\ c_{ab}^{a(a+1)},\ c_{ab}^{(b-1)b},\ \text{and } c_{ab}^{b(b+1)}.$$

For the remainder of this section, we will omit the subscript ab to ease the notation. Writing out $\mathrm{Q}_\xi 1$-$\mathrm{Q}_\xi 3$ for this fixed ab pair, we have six equations with six unknowns:

$$c^{aa} + c^{bb} + 2c^{(a-1)a} + 2c^{a(a+1)} + 2c^{(b-1)b} + 2c^{b(b+1)} = 2;$$

$$c^{aa}\mathbf{v}_{aa} + 2c^{(a-1)a}\mathbf{v}_{(a-1)a} + 2c^{a(a+1)}\mathbf{v}_{a(a+1)} + c^{bb}\mathbf{v}_{bb} + 2c^{(b-1)b}\mathbf{v}_{(b-1)b} + 2c^{b(b+1)}\mathbf{v}_{b(b+1)} = 2\mathbf{v}_{ab};$$

$$c^{aa}\mathbf{v}_a\mathbf{v}_a^T + c^{(a-1)a}(\mathbf{v}_{a-1}\mathbf{v}_a^T + \mathbf{v}_a\mathbf{v}_{a-1}^T) + c^{a(a+1)}(\mathbf{v}_a\mathbf{v}_{a+1}^T + \mathbf{v}_{a+1}\mathbf{v}_a^T) + c^{bb}\mathbf{v}_b\mathbf{v}_b^T + c^{(b-1)b}(\mathbf{v}_{b-1}\mathbf{v}_b^T + \mathbf{v}_b\mathbf{v}_{b-1}^T) + c^{b(b+1)}(\mathbf{v}_b\mathbf{v}_{b+1}^T + \mathbf{v}_{b+1}\mathbf{v}_b^T) = \mathbf{v}_a\mathbf{v}_b^T + \mathbf{v}_b\mathbf{v}_a^T.$$

Assume without loss of generality that $\mathbf{v}_a = (-\ell, 0)$ and $\mathbf{v}_b = (\ell, 0)$ with $\ell < 1/2$ (since Ω has diameter 1). We introduce the terms d_a and d_b defined by

$$d_a := \frac{(\mathbf{v}_{a-1})_x(\mathbf{v}_{a+1})_y - (\mathbf{v}_{a+1})_x(\mathbf{v}_{a-1})_y}{(\mathbf{v}_{a-1})_y - (\mathbf{v}_{a+1})_y} \cdot \frac{1}{\ell}, \text{ and} \tag{5.1}$$

$$d_b := \frac{(\mathbf{v}_{b+1})_x(\mathbf{v}_{b-1})_y - (\mathbf{v}_{b-1})_x(\mathbf{v}_{b+1})_y}{(\mathbf{v}_{b-1})_y - (\mathbf{v}_{b+1})_y} \cdot \frac{1}{\ell}. \tag{5.2}$$

These terms have a concrete geometrical interpretation as shown in Figure 5: $-d_a\ell$ is the x-intercept of the line between $\mathbf{v}_{a-1}$ and $\mathbf{v}_{a+1}$, while $d_b\ell$ is the x-intercept of the line between $\mathbf{v}_{b-1}$ and $\mathbf{v}_{b+1}$. Thus, by the convexity assumption, $d_a, d_b \in [-1, 1]$. Additionally, $-d_a \le d_b$ with equality only in the case of a quadrilateral which was dealt with previously. For ease of notation and subsequent explanation, we also define

$$s := \frac{2}{2 - (d_a + d_b)}. \tag{5.3}$$

First we choose $c^{(a-1)a}$ and $c^{a(a+1)}$ as the solution to the following system of equations:

$$c^{(a-1)a} + c^{a(a+1)} = s; \tag{5.4}$$

$$c^{(a-1)a}\mathbf{v}_{a-1} + c^{a(a+1)}\mathbf{v}_{a+1} = sd_a\mathbf{v}_a. \tag{5.5}$$

There are a total of three equations since (5.5) equates vectors, but it can be verified directly that this system of equations is only rank two. Moreover, any two of the equations from (5.4) and (5.5) suffice to give the same unique solution for $c^{(a-1)a}$ and $c^{a(a+1)}$.

Similarly, we select $c^{(b-1)b}$ and $c^{b(b-1)}$ as the solution to the system:

$$c^{(b-1)b} + c^{b(b+1)} = s; \tag{5.6}$$

$$c^{(b-1)b}\mathbf{v}_{b-1} + c^{b(b+1)}\mathbf{v}_{b+1} = sd_b\mathbf{v}_b. \tag{5.7}$$

Finally, we assign c^{aa} and c^{bb} by

$$c^{aa} = \frac{-2 - 2d_a}{2 - (d_a + d_b)} \text{ and} \tag{5.8}$$

$$c^{bb} = \frac{-2 - 2d_b}{2 - (d_a + d_b)}, \tag{5.9}$$

and claim that this set of coefficients leads to a basis with quadratic precision.

Lemma 5.1. *The coefficients defined by (5.4)-(5.9) satisfy constraints $Q_\xi 1$-$Q_\xi 3$.*

Proof. Observe that c^{aa}_{aa} and c^{bb}_{bb} satisfy the following equations:

$$c^{aa}_{aa} + c^{bb}_{bb} + 4s = 2; \tag{5.10}$$

$$c^{aa} - c^{bb} + s(d_a - d_b) = 0; \tag{5.11}$$

$$c^{aa} + c^{bb} + 2s(d_a + d_b) = -2. \tag{5.12}$$

They will be used to verify $Q_\xi 1$, $Q_\xi 2$, and $Q_\xi 3$, respectively. First, note that $Q_\xi 1$ follows immediately from (5.4), (5.6) and (5.10).

The linear precision property ($Q_\xi 2$) is just a matter of algebra. Equations (5.4)-(5.7) yield

$$\begin{aligned}
&c^{aa}\mathbf{v}_{aa} + c^{bb}\mathbf{v}_{bb} + 2c^{(a-1)a}\mathbf{v}_{(a-1)a} + 2c^{a(a+1)}\mathbf{v}_{a(a+1)} + 2c^{(b-1)b}\mathbf{v}_{(b-1)b} + 2c^{b(b+1)}\mathbf{v}_{b(b+1)} \\
&\quad = (c^{aa} + c^{(a-1)a} + c^{a(a+1)})\mathbf{v}_a + (c^{bb} + c^{(b-1)b} + c^{b(b+1)})\mathbf{v}_b \\
&\qquad + c^{(a-1)a}\mathbf{v}_{a-1} + c^{a(a+1)}\mathbf{v}_{a+1} + c^{(b-1)b}\mathbf{v}_{b-1} + c^{b(b+1)}\mathbf{v}_{b+1} \\
&\quad = (c^{aa} + c^{(a-1)a} + c^{a(a+1)})\mathbf{v}_a + (c^{bb} + c^{(b-1)b} + c^{b(b+1)})\mathbf{v}_b + sd_a\mathbf{v}_a + sd_b\mathbf{v}_b \\
&\quad = (c^{aa} + s + sd_a)\mathbf{v}_a + (c^{bb} + s + sd_b)\mathbf{v}_b.
\end{aligned}$$

Substituting the fixed coordinates of $\mathbf{v}_a$ and $\mathbf{v}_b$ reduces this expression to the vector

$$\begin{bmatrix} (-c^{aa} - s - sd_a + c^{bb} + s + sd_b)\ell \\ 0 \end{bmatrix}.$$

The x-coordinate is zero by (5.11). This proves $Q_\xi 2$, since $2\mathbf{v}_{ab} = \mathbf{v}_a + \mathbf{v}_b = \vec{0}$. Finally, we check quadratic precision. We factor the left side of $Q_\xi 3$ as follows:

$$\begin{aligned}
&c^{aa}\mathbf{v}_a\mathbf{v}_a^T + c^{bb}\mathbf{v}_b\mathbf{v}_b^T + c^{(a-1)a}(\mathbf{v}_{a-1}\mathbf{v}_a^T + \mathbf{v}_a\mathbf{v}_{a-1}^T) + \cdots + c^{b(b+1)}(\mathbf{v}_b\mathbf{v}_{b+1}^T + \mathbf{v}_{b+1}\mathbf{v}_b^T) \\
&\quad = c^{aa}\mathbf{v}_a\mathbf{v}_a^T + c^{bb}\mathbf{v}_b\mathbf{v}_b^T \\
&\qquad + (c^{(a-1)a}\mathbf{v}_{a-1} + c^{a(a+1)}\mathbf{v}_{a+1})\mathbf{v}_a^T + \mathbf{v}_a(c^{(a-1)a}\mathbf{v}_{a-1}^T + c^{a(a+1)}\mathbf{v}_{a+1}^T) \\
&\qquad + (c^{(b-1)b}\mathbf{v}_{b-1} + c^{b(b+1)}\mathbf{v}_{b+1})\mathbf{v}_b^T + \mathbf{v}_b(c^{(b-1)b}\mathbf{v}_{b-1}^T + c^{b(b+1)}\mathbf{v}_{b+1}^T) \\
&\quad = c^{aa}\mathbf{v}_a\mathbf{v}_a^T + c^{bb}\mathbf{v}_b\mathbf{v}_b^T + sd_a\mathbf{v}_a\mathbf{v}_a^T + sd_b\mathbf{v}_b\mathbf{v}_b^T + \mathbf{v}_a(sd_a\mathbf{v}_a^T) + \mathbf{v}_b(sd_b\mathbf{v}_b^T) \\
&\quad = (c^{aa} + 2sd_a)\mathbf{v}_a\mathbf{v}_a^T + (c^{bb} + 2sd_b)\mathbf{v}_b\mathbf{v}_b^T.
\end{aligned}$$

Again substituting the coordinates of $\mathbf{v}_a$ and $\mathbf{v}_b$, we obtain the matrix

$$\begin{bmatrix} \left(c^{aa} + 2sd_a + c^{bb} + 2sd_b\right)\ell^2 & 0 \\ 0 & 0 \end{bmatrix}.$$

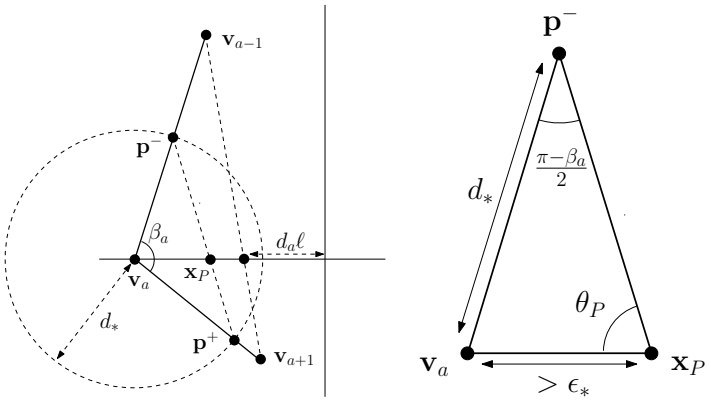

FIGURE 6. Notation used in proof of Theorem 5.3.

The right side of $\mathrm{Q}_\xi 3$ is

$$\mathbf{v}_a\mathbf{v}_b^T + \mathbf{v}_b\mathbf{v}_a^T = \begin{bmatrix} -2\ell^2 & 0 \\ 0 & 0 \end{bmatrix}.$$

Hence the only equation that must be satisfied is exactly (5.12). □

Remark 5.2. We note that s was specifically chosen so that (5.10)-(5.12) would hold. The case $s = 1$ happens when $d_a = -d_b$, i.e only for the quadrilateral.

Theorem 5.3. *Given a convex polygon satisfying G1, G2 and G3, $||\mathbb{A}||$ is uniformly bounded.*

Proof. It suffices to show a uniform bound on the six coefficients defined by equations (5.4)-(5.9). First we prove a uniform bound on d_a and d_b given G1-G3.

We fix some notation as shown in Figure 6. Let $C(\mathbf{v}_a, d_*)$ be the circle of radius d_* (from G2) around $\mathbf{v}_a$. Let $\mathbf{p}^- := (p_x^-, p_y^-)$ and $\mathbf{p}^+ := (p_x^+, p_y^+)$ be the points on $C(\mathbf{v}_a, d_*)$ where the line segments to $\mathbf{v}_a$ from $\mathbf{v}_{a-1}$ and $\mathbf{v}_{a+1}$, respectively, intersect. The chord on $C(\mathbf{v}_a, d_*)$ between $\mathbf{p}^-$ and $\mathbf{p}^+$ intersects the x-axis at $\mathbf{x}_p := (x_p, 0)$. By convexity, $(\mathbf{v}_a)_x < x_p$.

To bound $x_p - (\mathbf{v}_a)_x$ below, note that the triangle $\mathbf{v}_a\mathbf{p}^-\mathbf{p}^+$ with angle β_a at $\mathbf{v}_a$ is isosceles. Thus, the triangle $\mathbf{v}_a\mathbf{p}^-\mathbf{x}_p$ has angle $\angle\mathbf{v}_a\mathbf{p}^-\mathbf{x}_p = (\pi - \beta_a)/2$, as shown at the right of Figure 6. By the law of sines on this smaller triangle, we can write

$$x_p - (\mathbf{v}_a)_x = \frac{d_* \sin\left(\frac{\pi-\beta_a}{2}\right)}{\sin\theta_p}.$$

Note $p_x^-, p_x^+ > (\mathbf{v}_a)_x$, $p_y^- > 0$ and $p_y^+ < 0$ by convexity. Thus the angle $\theta_p := \angle\mathbf{v}_a x_p\mathbf{p}^- \in (\pi/4, \pi/2)$ meaning $\sin\theta_p > 0$. Based on G3, $\epsilon_* > 0$ is defined to be

$$x_p - (\mathbf{v}_a)_x > d_* \sin\left(\frac{\pi-\beta_a}{2}\right) > d_* \sin\left(\frac{\pi-\beta^*}{2}\right) =: \epsilon_* > 0. \tag{5.13}$$

Since $-d_a\ell < 1$ is the x-intercept of the line between $\mathbf{v}_{a-1}$ and $\mathbf{v}_{a+1}$, we have $x_p \le -d_a\ell$. Then we rewrite $(\mathbf{v}_a)_x = -\ell$ in the geometrically suggestive form

$$(x_p - (\mathbf{v}_a)_x) + (-d_a\ell - x_p) + (0 + d_a\ell) = \ell.$$

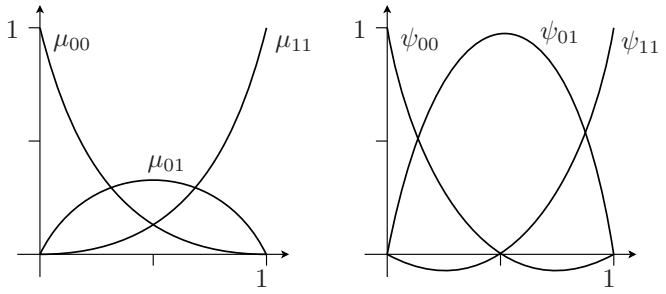

FIGURE 7. A comparison of the product barycentric basis (left) with the standard Lagrange basis (right) for quadratic polynomials in one dimension.

Since $-d_a\ell - x_p \geq 0$, we have $\mathbf{x}_p - (\mathbf{v}_a)_x + d_a\ell \leq \ell$. Using (5.13), this becomes $d_a\ell < \ell - \epsilon_*$. Recall from Figure 5 and previous discussion that $d_a, d_b \in [-1, 1]$ and $-d_a \leq d_b$. By symmetry, $d_b\ell < \ell - \epsilon_*$ and hence $d_a + d_b < 2\ell - 2\epsilon_* < 1 - 2\epsilon_*$.

We use the definition of c^{aa} from (5.8), the derived bounds on d_a and d_b, and the fact that $\ell \leq 1/2$ to conclude that

$$|c^{aa}| < \frac{|2 + 2d_a|}{1 + 2\epsilon_*} < \frac{2 + 2(1 - (\epsilon_*/\ell))}{1 + 2\epsilon_*} \leq \frac{4 - 4\epsilon_*}{1 + 2\epsilon_*} < 4.$$

Similarly, $|c^{bb}| < \frac{4-4\epsilon_*}{1+2\epsilon_*} < 4$. For the remaining coefficients, observe that the definition of s in (5.3) implies that $0 < s < 2/(1 + 2\epsilon_*)$. Equation (5.4) and the y-component of equation (5.5) ensure that $c^{(a-1)a}/s$ and $c^{a(a+1)}/s$ are the coefficients of a convex combination of $\mathbf{v}_{a-1}$ and $\mathbf{v}_{a+1}$. Thus $c^{(a-1)a}, c^{(a+1)a} \in (0, s)$ and s serves as an upper bound on the norms of each coefficient. Likewise, $|c^{(b-1)b}|, |c^{b(b+1)}| < s$. Therefore,

$$\max\left(\frac{4 - 4\epsilon_*}{1 + 2\epsilon_*}, \frac{2}{1 + 2\epsilon_*}, 1\right)$$

is a uniform bound on all the coefficients of $\mathbb{A}$. □

6. Conversion to a Lagrange-like Basis

The set of $2n$ basis functions constructed thus far naturally corresponds to vertices and edges of the polygon, but the functions associated to midpoints are not Lagrange-like at any points. This is because the functions of the form $\xi_{i(i+1)}$ may not evaluate to 1 at $\mathbf{v}_{i(i+1)}$, even though the set of $\{\xi_{ij}\}$ satisfies the partition of unity property $\mathrm{Q}_\xi 1$. The remedy turns out to be a simple bounded linear transformation given by the matrix $\mathbb{B}$ defined below.

To motivate our approach, we first consider a simpler setting: polynomial bases over the unit segment $[0, 1] \subset \mathbb{R}$. The barycentric functions on this domain are $\lambda_0(x) = 1 - x$, and $\lambda_1(x) = x$. Taking pairwise products, we get the quadratic basis $\mu_{00}(x) := (\lambda_0(x))^2 = (1 - x)^2$, $\mu_{01}(x) := \lambda_0(x)\lambda_1(x) = (1 - x)x$, and $\mu_{11}(x) := (\lambda_1(x))^2 = x^2$, shown on the left of Figure 7. This basis is not Lagrange-like since $\mu_{01}(1/2) \neq 1$ and $\mu_{00}(1/2), \mu_{11}(1/2) \neq 0$. The quadratic Lagrange basis is given by $\psi_{00}(x) := (1 - x)\left(\frac{1}{2} - x\right)$, $\psi_{01}(x) := 4(1 - x)x$, and $\psi_{11}(x) := 2\left(x - \frac{1}{2}\right)x$, shown on the right of Figure 7. These two bases are related by the linear transformation

$\mathbb{B}_{1D}$:

$$[\psi_{ij}] = \begin{bmatrix}\psi_{00}\\ \psi_{01}\\ \psi_{11}\end{bmatrix} = \begin{bmatrix}1 & 0 & -1\\ 0 & 1 & -1\\ 0 & 0 & 4\end{bmatrix}\begin{bmatrix}\mu_{00}\\ \mu_{01}\\ \mu_{11}\end{bmatrix} = \mathbb{B}_{1D}[\mu_{ij}]. \tag{6.1}$$

This procedure generalizes to the case of converting the 2D serendipity basis $\{\xi_{ij}\}$ to a Lagrange like basis $\{\psi_{ij}\}$. Define

$$\psi_{ii} := \xi_{ii} - \xi_{i,i+1} - \xi_{i-1,i} \quad \text{and} \quad \psi_{i,i+1} = 4\xi_{i,i+1}.$$

The transformation matrix $\mathbb{B}$ has the structure

$$[\psi_{ij}] = \begin{bmatrix}\psi_{11}\\ \psi_{22}\\ \vdots\\ \psi_{nn}\\ \psi_{12}\\ \psi_{23}\\ \vdots\\ \psi_{1n}\end{bmatrix} = \left[\begin{array}{cccc|cccccc} 1 & & & & -1 & & \cdots & & & -1\\ & 1 & & & -1 & -1 & \cdots & & & \\ & & \ddots & & & \ddots & \ddots & & & \\ & & & \ddots & & & \ddots & \ddots & & \\ & & & 1 & & & & -1 & -1 & \\ \hline & & & & 4 & & & & & \\ & & & & & 4 & & & & \\ & & 0 & & & & \ddots & & & \\ & & & & & & & \ddots & & \\ & & & & & & & & 4 & \end{array}\right]\begin{bmatrix}\xi_{11}\\ \xi_{22}\\ \vdots\\ \xi_{nn}\\ \xi_{12}\\ \xi_{23}\\ \vdots\\ \xi_{1n}\end{bmatrix} = \mathbb{B}[\xi_{ij}].$$

The following proposition states precisely what it means to say the functions $\{\psi_{ij}\}$ are Lagrange-like.

Proposition 6.1. For all $i, j \in \{1, \ldots, n\}$, $\psi_{ii}(\mathbf{v}_j) = \delta_i^j$, $\psi_{ii}(\mathbf{v}_{j,j+1}) = 0$, $\psi_{i,i+1}(\mathbf{v}_j) = 0$, and $\psi_{i,i+1}(\mathbf{v}_{j,j+1}) = \delta_i^j$.

In closing, note that $||\mathbb{B}||$ is uniformly bounded since its entries all lie in $\{-1, 0, 1, 4\}$.

7. Applications and Extensions

Our quadratic serendipity element construction has a number of uses in modern finite element application contexts. First, the construction for quadrilaterals given in Section 4.2 allows for quadratic order methods on *arbitrary* quadrilateral meshes with only eight basis functions per element instead of the nine required by traditional methods permitting greater flexibility in domain meshing without substantial increase in computational cost. This result contrasts with the the standard bilinear quadrilateral element for which no eight-node construction can yield the desired error estimate [4].

To demonstrate the success of our approach, we use our construction to solve Poisson's equation on a square domain using convex quadrilateral elements. Meshing the domain with n^2 trapezoidal elements as shown in Figure 8(left) is known to produce sub-quadratic convergence when traditional serendipity elements are used [4]. We prescribe boundary conditions corresponding to the solution $u(x, y) = \sin(x)e^y$ and use our construction from Section 4.2, starting with mean value coordinates [12] for the λ_i functions. As shown in Figure 8(right), the expected convergence rates from our theoretical analysis are observed, namely, cubic in the L^2-norm and quadratic in the H^1-norm.

An additional application of our method is to adaptive finite elements, such as the one shown in Figure 9. This is possible since the result of Theorem 5.3 still holds if G3 fails to hold only on a set of consecutive vertices of the polygon. This weakened condition suffices since consecutive large angles in the polygon do not cause the coefficients c_{ab}^{ij} to blow up. For instance, consider the degenerate pentagon shown in Figure 9 which satisfies this weaker condition but not G3. Examining the potentially problematic coefficients c_{25}^{ij}, it is easily confirmed that $d_a = d_b = 0$ and hence $s = 1$. Thus, the analysis from the proof of Theorem 5.3 holds as stated for these coefficients and hence for the entire element. A more detailed analysis of such large-angle elements is an open question for future study.

Non-consecutive large angles as well as very short edges, however, can present a problem for our construction. Figure 10 shows examples of shapes not suited to the method we have described. In the left figure, as edges $\mathbf{v}_{a-1}\mathbf{v}_a$ and $\mathbf{v}_{b-1}\mathbf{v}_b$ approach length zero, d_a and d_b both approach one meaning s (in the construction of Section 5) approaches ∞. In this case, the coefficients $c_{ij}^{(a-1)a}$ and $c_{ij}^{(b-1)b}$ grow larger without bound, thereby violating the result of Theorem 5.3. In the right figure, as the overall shape approaches a square, d_a and d_b again approach one so that s again approaches ∞. In this case, all the coefficients $c_{ij}^{(a-1)a}$, $c_{ij}^{a(a+1)}$, $c_{ij}^{(b-1)b}$ and $c_{ij}^{b(b+1)}$ all grow without bound. Nevertheless, if these types of extreme geometries are required, it may be possible to devise alternative definitions of the c_{ij}^{ab} coefficients satisfying $\mathrm{Q}_\xi 1$-$\mathrm{Q}_\xi 3$ with controlled norm estimates since the set of restrictions $\mathrm{Q}_\xi 1$-$\mathrm{Q}_\xi 3$ does not have full rank. (Note that this flexibility has lead to multiple constructions of the traditional serendipity square [23, 21]). Cursory numerical experimentation suggests that some bounded construction exists even in the degenerate situation.

Finally, we note that although this construction is specific to quadratic elements, the approach seems adaptable, with some effort, to the construction of cubic and higher order serendipity elements on generic convex polygons. As a larger linear

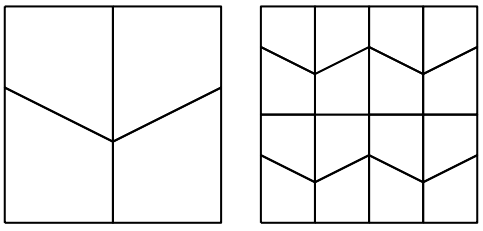

	$\|\|u - u_h\|\|_{L^2}$		$\|\|\nabla(u - u_h)\|\|_{L^2}$	
n	error	rate	error	rate
2	2.34e-3		2.22e-2	
4	3.03e-4	2.95	6.10e-3	1.87
8	3.87e-5	2.97	1.59e-3	1.94
16	4.88e-6	2.99	4.04e-4	1.97
32	6.13e-7	3.00	1.02e-4	1.99
64	7.67e-8	3.00	2.56e-5	1.99
128	9.59e-9	3.00	6.40e-6	2.00
256	1.20e-9	3.00	1.64e-6	1.96

FIGURE 8. Trapezoidal meshes (left) fail to produce quadratic convergence with traditional serendipity elements; see [4]. Since our construction begins with affinely-invariant generalized barycentric functions, the expected quadratic convergence rate can be recovered (right). The results shown were generated using the basis $\{\psi_{ij}\}$ resulting from the selection of the mean value coordinates as the initial barycentric functions.

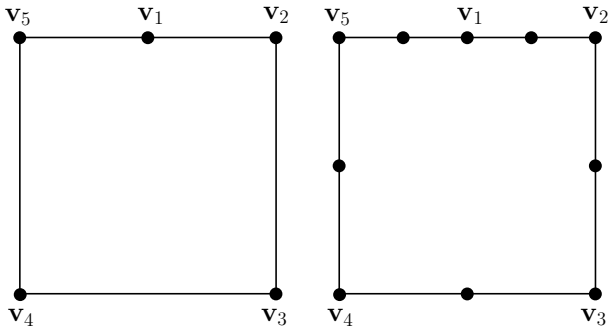

FIGURE 9. The degenerate pentagon (left), widely used in adaptive finite element methods for quadrilateral meshes, satisfies G1 and G2, but only satisfies G3 for four of its vertices. The bounds on the coefficients c_{ab}^{ij} from Section 5 still hold, however, meaning our approach can be applied to this element, resulting in the Lagrange-like quadratic element (right).

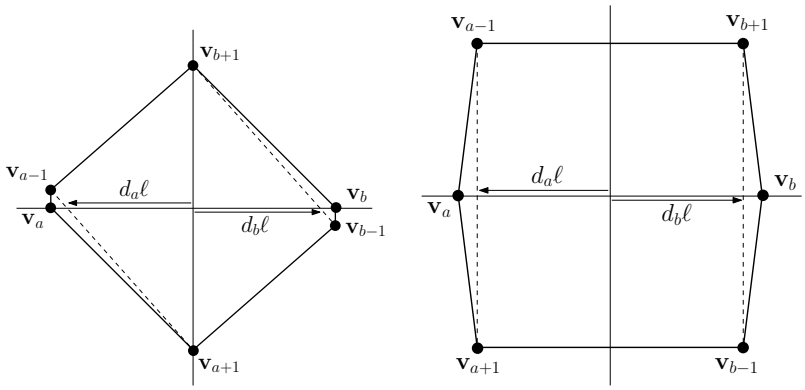

FIGURE 10. Examples of shapes showing the necessity of G2 and G3 for the results of Theorem 5.3.

system must be satisfied, stating an explicit solution becomes complex. Further research along these lines should probably assert the existence of a uniformly bounded solution without specifying the construction. In practice, a least squares solver can be used to construct the basis numerically.

REFERENCES

1. D. Apprato, R. Arcanceli, and J. L. Gout, *Rational interpolation of Wachspress error estimates*, Computers & Mathematics with Applications **5** (1979), no. 4, 329–336.
2. D. Apprato, R. Arcangeli, and J. L. Gout, *Sur les elements finis rationnels de Wachspress*, Numerische Mathematik **32** (1979), no. 3, 247–270.
3. D. N. Arnold and G. Awanou, *The serendipity family of finite elements*, Foundations of Computational Mathematics **11** (2011), no. 3, 337–344.
4. D. N. Arnold, D. Boffi, and R. S. Falk, *Approximation by quadrilateral finite elements*, Mathematics of Computation **71** (2002), no. 239, 909–922.
5. S. C. Brenner and L. R. Scott, *The mathematical theory of finite element methods*, third ed., Texts in Applied Mathematics, vol. 15, Springer, New York, 2008. MR 2373954 (2008m:65001)

6. S. H. Christiansen, *A construction of spaces of compatible differential forms on cellular complexes*, Math. Models Methods Appl. Sci. **18** (2008), no. 5, 739–757.
7. P. G. Ciarlet, *The finite element method for elliptic problems*, second ed., Classics in Applied Mathematics, vol. 40, SIAM, Philadelphia, PA, 2002.
8. E. Cueto, N. Sukumar, B. Calvo, M. A. Martínez, J. Cegoñino, and M. Doblaré, *Overview and recent advances in natural neighbour Galerkin methods*, Arch. Comput. Methods Engrg. **10** (2003), no. 4, 307–384. MR 2032470 (2004m:65190)
9. S. Dekel and D. Leviatan, *The Bramble-Hilbert lemma for convex domains*, SIAM Journal on Mathematical Analysis **35** (2004), no. 5, 1203–1212.
10. A. Ern and J.-L. Guermond, *Theory and practice of finite elements*, Applied Mathematical Sciences, vol. 159, Springer-Verlag, New York, 2004. MR 2050138 (2005d:65002)
11. G. Farin, *Surfaces over Dirichlet tessellations*, Computer Aided Geometric Design **7** (1990), no. 1-4, 281–292.
12. M. Floater, *Mean value coordinates*, Computer Aided Geometric Design **20** (2003), no. 1, 19–27.
13. M. Floater, K. Hormann, and G. Kós, *A general construction of barycentric coordinates over convex polygons*, Advances in Computational Mathematics **24** (2006), no. 1, 311–331.
14. A. Gillette and C. Bajaj, *A generalization for stable mixed finite elements*, Proceedings of the 14th ACM Symposium of Solid and Physical Modeling, 2010, pp. 41–50.
15. ———, *Dual formulations of mixed finite element methods with applications*, to appear in Computer Aided Design (2011), arXiv:1012.3929 [math.DG].
16. A. Gillette, A. Rand, and C. Bajaj, *Error estimates for generalized barycentric coordinates*, to appear in Advances in Computational Mathematics (2011), arXiv:1010.5005 [math.NA].
17. J. L. Gout, *Construction of a Hermite rational "Wachspress type" finite element*, Computers & Mathematics with Applications **5** (1979), no. 4, 337–347.
18. ———, *Rational Wachspress-type finite elements on regular hexagons*, IMA Journal of Numerical Analysis **5** (1985), no. 1, 59.
19. T. Hughes, *The finite element method*, Prentice Hall Inc., Englewood Cliffs, NJ, 1987, Linear static and dynamic finite element analysis, With the collaboration of Robert M. Ferencz and Arthur M. Raefsky.
20. P. Joshi, M. Meyer, T. DeRose, B. Green, and T. Sanocki, *Harmonic coordinates for character articulation*, ACM Transactions on Graphics **26** (2007), 71.
21. F. Kikuchi, M. Okabe, and H. Fujio, *Modification of the 8-node serendipity element*, Comput. Methods Appl. Mech. Engrg. **179** (1999), no. 1-2, 91–109.
22. T. Langer and H.P. Seidel, *Higher order barycentric coordinates*, Computer Graphics Forum, vol. 27, 2008, pp. 459–466.
23. R. H. MacNeal and R. L. Harder, *Eight nodes or nine?*, International Journal for Numerical Methods in Engineering **33** (1992), no. 5, 1049–1058.
24. S. Martin, P. Kaufmann, M. Botsch, M. Wicke, and M. Gross, *Polyhedral finite elements using harmonic basis functions*, SGP '08: Proceedings of the Symposium on Geometry Processing (Aire-la-Ville, Switzerland), Eurographics Association, 2008, pp. 1521–1529.
25. P. Milbradt and T. Pick, *Polytope finite elements*, International Journal for Numerical Methods in Engineering **73** (2008), no. 12, 1811–1835.
26. M. M. Rashid and M. Selimotic, *A three-dimensional finite element method with arbitrary polyhedral elements*, International Journal for Numerical Methods in Engineering **67** (2006), no. 2, 226–252.
27. R. Sibson, *A vector identity for the Dirichlet tessellation*, Math. Proc. Cambridge Philos. Soc. **87** (1980), no. 1, 151–155.
28. D. Sieger, P. Alliez, and M. Botsch, *Optimizing voronoi diagrams for polygonal finite element computations*, Proc. 19th Int. Meshing Roundtable (2010), 335–350.
29. G. Strang and G. J. Fix, *An analysis of the finite element method*, Prentice-Hall Inc., Englewood Cliffs, N. J., 1973, Prentice-Hall Series in Automatic Computation.
30. N. Sukumar and E. A. Malsch, *Recent advances in the construction of polygonal finite element interpolants*, Archives of Computational Methods in Engineering **13** (2006), no. 1, 129–163.
31. N. Sukumar and A. Tabarraei, *Conforming polygonal finite elements*, International Journal for Numerical Methods in Engineering **61** (2004), no. 12, 2045–2066.
32. A. Tabarraei and N. Sukumar, *Application of polygonal finite elements in linear elasticity*, International Journal of Computational Methods **3** (2006), no. 4, 503–520.

33. R. Verfürth, *A note on polynomial approximation in Sobolev spaces*, Mathematical Modelling and Numerical Analysis **33** (1999), no. 4, 715–719.
34. E. L. Wachspress, *A rational finite element basis*, Mathematics in Science and Engineering, vol. 114, Academic Press, New York, 1975.
35. M. Wicke, M. Botsch, and M. Gross, *A finite element method on convex polyhedra*, Computer Graphics Forum **26** (2007), no. 3, 355–364.
36. J. Zhang and F. Kikuchi, *Interpolation error estimates of a modified 8-node serendipity finite element*, Numer. Math. **85** (2000), no. 3, 503–524.
37. O. Zienkiewicz and R. Taylor, *The finite element method*, fifth ed., Butterworth-Heinemann, London, 2000.

Institute for Computational Engineering and Sciences, The University of Texas at Austin
E-mail address: arand@ices.utexas.edu

Department of Mathematics, The University of Texas at Austin
E-mail address: agillette@math.utexas.edu

Department of Computer Science, The University of Texas at Austin
E-mail address: bajaj@cs.utexas.edu